engineering proceedings

MDPI

Proceeding Paper

Simulation and Experimental Investigation of an SRM Drive in Motoring Mode †

Tsvetana Grigorova [1,*], Georgi Bodurov [1] and Dimitar Yankov [1,2]

[1] Department of Electronics, Faculty of Electronics and Automation, Technical University of Sofia, Plovdiv Branch, 63 Sankt Petersburg Blvd., 4000 Plovdiv, Bulgaria; gbodurov@tu-plovdiv.bg (G.B.); d.yankov@tu-plovdiv.bg (D.Y.)

[2] Center of Competence "Smart Mechatronic, Eco-, and Energy-Saving Systems and Technologies", 4000 Plovdiv, Bulgaria

* Correspondence: c_gr@tu-plovdiv.bg

† Presented at the 15th International Scientific Conference TechSys 2026—Engineering, Technologies and Systems, Plovdiv, Bulgaria, 14–16 May 2026.

Abstract

The paper presents a simulation and experimental study of a three-phase 12/8 Switched Reluctance Motor (SRM) operating in motoring mode. The operation of the asymmetric bridge converter is analyzed, and the mathematical equations describing the phase-current change under various commutation states in soft-switching mode (modulation of the upper transistors) are derived. An analytical model is used to examine the energy exchange between the battery, the power switches, and the phase inductance. For the purposes of the study, a simulation model was developed in the MATLAB/Simulink R2025b environment, including models of the battery, the power converter, and the SRM. Simulation studies were conducted under various load conditions and phase current values, yielding time-domain waveforms of the phase currents and voltages, as well as the electromagnetic torque. Experimental waveforms of the phase current and voltage, measured under conditions corresponding to those in the simulation studies, are presented. A comparative analysis was performed between the simulation and experimental results, with tabular and graphical dependencies presented, and the relative error between them determined. The results obtained show good agreement between the simulation model and the actual system, which confirms the applicability of the developed approach for the analysis and optimization of SRM drives.

Keywords: Switched Reluctance Motor (SRM); asymmetric bridge converter; motoring mode PWM control

Check for updates

Academic Editors: Nikola G. Shakev, Valyo N. Nikolov, Nikolay R. Kakanakov and Sevil A. Ahmed-Shieva

Published: 17 July 2026

Copyright: © 2026 by the authors. Licensee MDPI, Basel, Switzerland. This article is an open access article distributed under the terms and conditions of the Creative Commons Attribution (CC BY) license.

1. Introduction

Switched reluctance motors (SRMs) have attracted significant interest from the scientific community due to their simple, robust design, high reliability, and ability to operate effectively across a wide range of loads and temperature conditions [1]. Recent studies emphasize that SRMs are particularly suitable for electric and hybrid vehicles because they do not use permanent magnets, resulting in high durability and a long service lifetime [2,3]. Despite these advantages, controlling these motors remains challenging because of the nonlinear relationships among phase inductance, phase current, and rotor position, which require specialized power converters.

The asymmetric bridge converter is the most common converter topology used to drive SRMs, as it allows for independent switching of individual phases, rapid regulation of

phase current, and the capability to return energy in generating mode. Detailed models and analyses of this topology are presented in the current scientific literature, including studies on the switching of power devices, losses, and the interaction among the battery. switching elements, and phase inductance [4,5]. Particular attention is given to the soft-switching mode, which reduces switching losses and torque ripples and improves drive efficiency [6].

Phase current control is a critical factor in generating electromagnetic torque and ensuring SRM drive operation under various operating conditions. Recent scientific studies indicate that PWM control and the optimization of on–off angles can significantly reduce torque ripple and improve the performance of the electric drive system [7]. However, the accuracy of the simulation study and the mathematical model depends on accurate measurement of the machine's nonlinear phase inductance profile and on the proper configuration of the power converter, which necessitates validation through experimental measurements.

The MATLAB/Simulink environments provide powerful tools for modeling SRMs and power electronic circuits, including built-in blocks for SRMs and converters. However, real electric drive systems often deviate from idealized models due to parasitic parameters, switching losses, and battery behavior.

This study investigates the operation of a three-phase 12/8 switched reluctance motor (SRM) drive controlled by pulse width modulation (PWM) in motoring mode. A mathematical model of the processes in the asymmetric bridge converter is developed and used to perform simulations in MATLAB/Simulink, complemented by experimental investigations. Measurements of the RMS phase currents and voltages, generated torque, output power, and efficiency of the machine are carried out. A comparative analysis between simulation and experimental results is performed, and the relative error is evaluated to assess the accuracy of the proposed model. The results demonstrate that the developed model provides sufficient accuracy and can be effectively applied for control optimization and improvement of the energy efficiency of SRM drives.

2. Operation Principle

For the purposes of this study, a detailed analysis of electromagnetic processes in the asymmetric bridge converter and in the SRM phase winding under unipolar modulation was performed, implemented by switching the upper transistor. It is assumed that during the period in which the respective phase is turned on, the electromotive force has reached a steady state and can be considered a quantity with an approximately constant value. On this basis, equivalent circuit models are formulated that reflect the actual electromagnetic behavior of the phase under the various switching states.

The asymmetric bridge circuit is shown in Figure 1 [1–4]. A three-phase 12/8 Switched Reluctance Motor (SRM) is used during the simulation and experimental study. The initial condition in the analysis is taken to be the turn-on of transistors M1 and M2. This approach allows evaluation of the influence of unipolar modulation on the current and voltage, as well as on the magnetization in the machine.

When operating in motoring mode, phase switching occurs in the region of increasing inductance, i.e., when $\left(dL_{ph}/d\theta_{ph} > 0\right)$. The waveforms illustrating the operation of an asymmetric bridge converter–SRM in motoring mode under "soft switching" (unipolar modulation) are shown in Figure 2.

The equivalent circuit diagrams of the asymmetric bridge converter in the modes where two transistors are on, the upper transistor is modulated, and the upper and lower transistors are off are shown in Figure 3a–c [8,9].

https://doi.org/10.3390/engproc2026150012

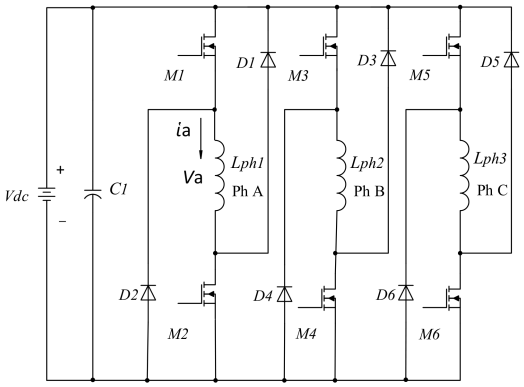


Figure 1. Asymmetric bridge converter for the three-phase SRM.

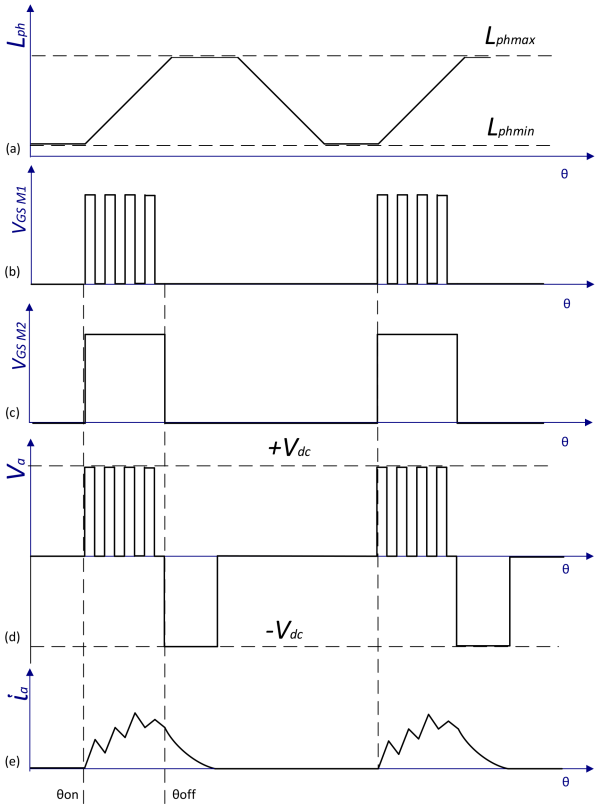


Figure 2. Waveforms of an asymmetric bridge converter with soft switching: (**a**) ideal phase inductance L_{ph}; (**b**) control signals for M1 $V_{GS\ M1}$; (**c**) control signals for M2 $V_{GS\ M2}$; (**d**) phase voltage Va; (**e**) phase current i_a.

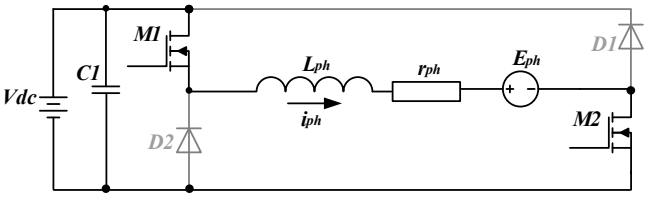
Transistors M1 and M2 (phase A) are turned on during the conduction period with a duty cycle D, after which M1 is turned off for an interval with a duty cycle $D' = 1 - D$. Both transistors are completely turned off at an angle θ_{off}. In this mode, the asymmetric bridge converter is treated as a step-down converter, with the current and voltage processes governed by it.

Assuming that the phase inductance can be described by an idealized profile (Figure 2a), the phase current i_{ph} is described by the following relationships [1]:

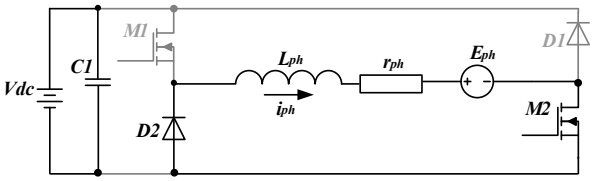
$$i_{ph} = \frac{\Psi_{ph}}{L_{ph}\left(\theta_{ph}\right)} = \begin{cases} \frac{V_{dc}\left(\theta_{ph}-\theta_{on}\right)}{\omega L_{ph}\left(\theta_{ph}\right)}, & \theta_{on} < \theta_{ph} < \theta_{off} \\ I_{ph}, & \theta_{off} < \theta_{ph} < \theta_{d} \end{cases} \quad (1)$$

$$i_{ph} = \frac{\Psi_{ph}}{L_{ph}\left(\theta_{ph}\right)} = \begin{cases} \frac{V_{dc}\left(\theta_{ph}-\theta_{on}\right)}{\omega L_{ph}\left(\theta_{ph}\right)}, & \theta_{on} < \theta_{ph} < \theta_{off} \\ I_{ph}, & \theta_{off} < \theta_{ph} < \theta_{d} \end{cases} \quad (2)$$

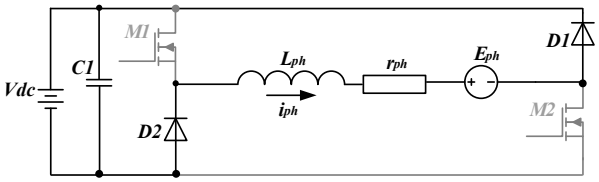
where I_{ph} is the value of the phase current during the period when the two transistors are turned off, V_{dc} is the supply voltage, ω is the angular velocity of the machine, θ_{on} and θ_{off} are the turn-on and the turn-off angles and θ_d is the dwell angle.



(**a**)



(**b**)



(**c**)

Figure 3. Equivalent circuit for the operation of the asymmetric circuit in motoring modes: (**a**) excitation—transistors M1 and M2 are on; (**b**) modulated upper transistor M1; (**c**) transistors are off.

The phase voltage $V_{phL_{ph}}\left(\theta_{ph}\right)$ in the different intervals is given by the following:

- In excitation mode, transistors M1 and M2 are turned on,

$$V_{phL_{ph}1}(\theta_{ph}) = V_{dc} - r_{ph}i_{ph} - E_{ph} \quad (3)$$

- M1 is turned off and M2 turned on,

$$V_{phL_{ph}2}\left(\theta_{ph}\right) = -E_{ph} - r_{ph}i_{ph} \quad (4)$$

- The transistors are off and diodes D1 and D2 are conducting,

$$V_{phL_{ph}3}\left(\theta_{ph}\right) = -E_{ph} - r_{ph}i_{ph} - V_{dc} \quad (5)$$

where E_{ph} is the back-EMF and r_{ph} is the stator resistance.

The average value of the voltage across the inductor in steady state over one cycle must be zero:

$$\frac{1}{\omega}\int_{\theta_{on}}^{\theta_{off}} \left(V_{phL_{ph}1}(\theta_{ph}) + V_{phL_{ph}2}(\theta_{ph}) + V_{phL_{ph}3}(\theta_{ph})\right)d\theta_{ph} = 0 \quad (6)$$

Since the excitation occurs in the lower region of the inductance profile, $L_{ph}\left(\theta_{ph}\right)$ is equal to its minimum value, L_{phmin}, and $E_{ph} = 0$ at the end of the phase conduction period. Therefore, (6) can be expressed as:

https://doi.org/10.3390/engproc2026150012

$$\frac{1}{\omega}\sum_{k_X}^{k}\left[\left(V_{dc}-r_{ph}i_{ph}-E_{ph}\right)\left(D\frac{k_X\Delta\theta_1}{k}\right)\right]+\sum_{k_x=1}^{k}\left[\left(-E_{ph}-r_{ph}i_{ph}\right)\left((1-D)\frac{k_X\Delta\theta_1}{k}\right)\right]+ \\ +\int_{\theta_{off}}^{\theta_d}\left(-E_{ph}-r_{ph}i_{ph}-V_{dc}\right)d\theta_{ph}=0. \tag{7}$$

where $\Delta\theta_1=\theta_{off}-\theta_{on}$ is the duration of the phase and $k=\Delta\theta_1/\omega T_{SW}$.

After rearrangement, (7) is given by

$$\sum_{k_X}^{k}\left[\left(V_{dc}-r_{ph}i_{ph}-E_{ph}\right)D+\left(-E_{ph}-r_{ph}i_{ph}\right)D'\right]\Delta\theta_1+ \\ +\left(-V_{dc}\Delta\theta_2\left(1+\frac{r_{ph}\Delta\theta_2}{\omega L_{phmax}}\right)\right)=0 \tag{8}$$

Expression (8) is written as follows:

$$\left(V_{dc}D-E_{ph}-\frac{k+1}{2}r_{ph}i_{ph}\right)\Delta\theta_1-V_{dc}\,\Delta\theta_2\left(1+\frac{r_{ph}\,\Delta\theta_2}{2\,\omega L_{phmax}}\right)=0 \tag{9}$$

where $\Delta\theta_2=\theta_d-\theta_{off}$ is the interval of energy generation, and $\sum_{k_x=1}^{k}\frac{k_x}{k}=\left(\frac{k+1}{2}\right)$.

The average value of the current through the capacitor in steady state over one cycle must be zero and is given by the following equation:

$$\frac{1}{T}\int_0^T i_C(t)dt=0 \tag{10}$$

After substituting the current values for the three switching modes of the transistors, (5) can be written as:

$$\sum_{k_x=1}^{k}\left[\left(I_{dc}-i_{ph}\right)D\,\frac{k_x\Delta\theta_1}{k}\right]+\sum_{k_x=1}^{k}\left[I_{dc}(1-D)\frac{k_x\Delta\theta_1}{k}\right]+\int_{\theta_{off}}^{\theta_d}\left(I_{dc}+i_{ph}\right)d\theta_{ph}=0 \tag{11}$$

The analysis shows that unipolar modulation significantly affects the shape of the phase current, the phase voltage, and the phase magnetization in the asymmetric bridge converter. Modulation of the upper transistor leads to smoother current control and reduced switching losses, which are essential for the efficient operation of the SRM in drive mode. The analytical relationships obtained form the basis for developing the simulation model and for comparing it with experimental studies.

3. Simulation and Experimental Study of the Operation of the System in Motoring Mode Under PWM Control

This section presents a simulation and experimental study of the system's motoring mode operation under pulse-width modulation (PWM) control, along with a comparative analysis of the results. The oscillograms of the phase voltages and currents obtained through simulation and experiment were compared to estimate the correspondence between the mathematical model and the actual system and to identify the characteristic features of the electromagnetic processes under unipolar modulation.

To ensure a comprehensive analysis, the system was studied under various load conditions and speeds. The results are presented in tabular and graphical form. Analyzing the presented dependencies allows for a quantitative assessment of the relative errors between the simulation and experimental results. This enables the determination of the accuracy of the developed model and the influence of various parameters on the electric drive's operation.

3.1. Control System Operation

The schematic diagram of the electric drive system under study, with the upper-transistor modulation in the MATLAB/Simulink environment, is shown in Figure 4. The corresponding power switches are controlled by a PWM generator based on the position of the machine's rotor. The duty cycle and frequency settings are fixed and do not change over time.

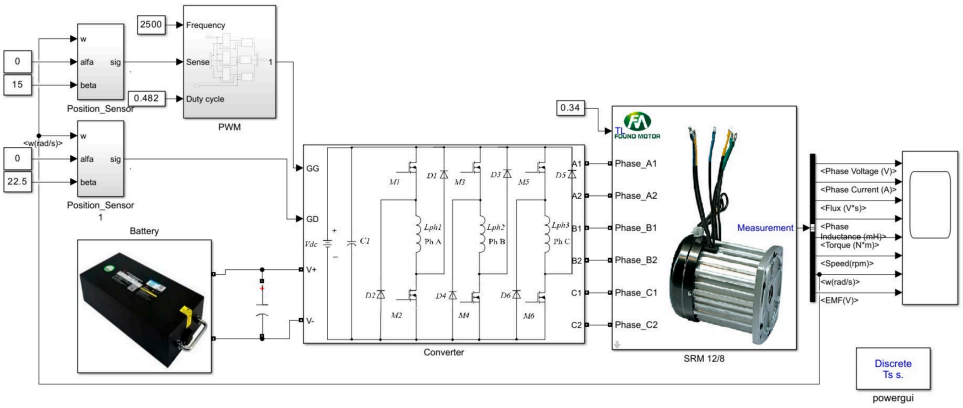
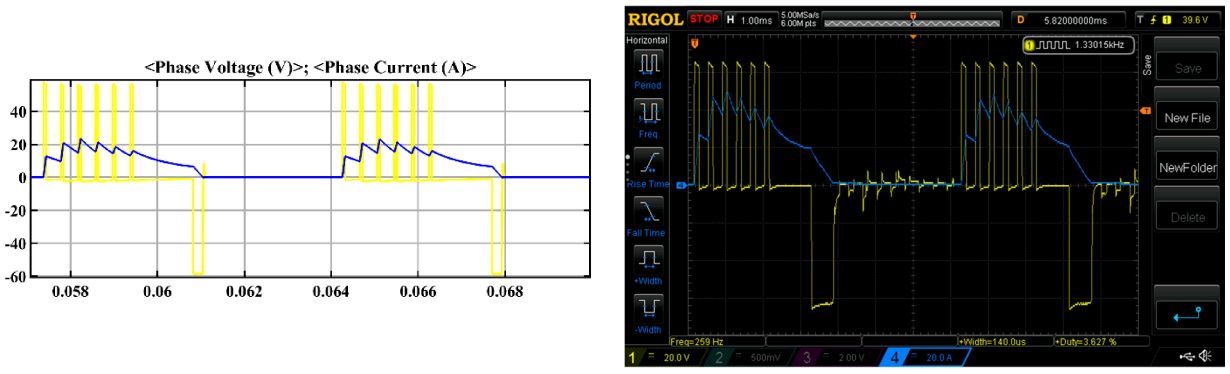


Figure 4. Simulink schematic diagram of a 12/8-type three-phase SRM controlled via PWM and soft commutation.

The simulation and experimental results obtained for the control system under study using single-pulse modulation are presented. To ensure the reliability of these results, the control algorithm was implemented in the same way as in the experimental setup. The machine operates in motoring mode with the following input parameters: PWM duty cycle D = 0.15; motor speed n = 1100 rpm; switching frequency of the upper transistors f = 2.5 kHz; turn-on angle for the upper and lower transistors $\theta_{on} = 0°$; turn-off angle for the upper transistors $\theta_{upoff} = 15°$; and turn-off angle for the lower transistors $\theta_{downoff} = 22.5°$, with a load torque TL = 0.77 Nm. A battery comprising 16 Li-ion cells connected in series, with a nominal voltage of 3.71 V, supplies power to the electric drive system.

The waveforms illustrating the simulation and experimental results for the phase voltage (yellow) and current (blue) are shown in Figure 5a,b.

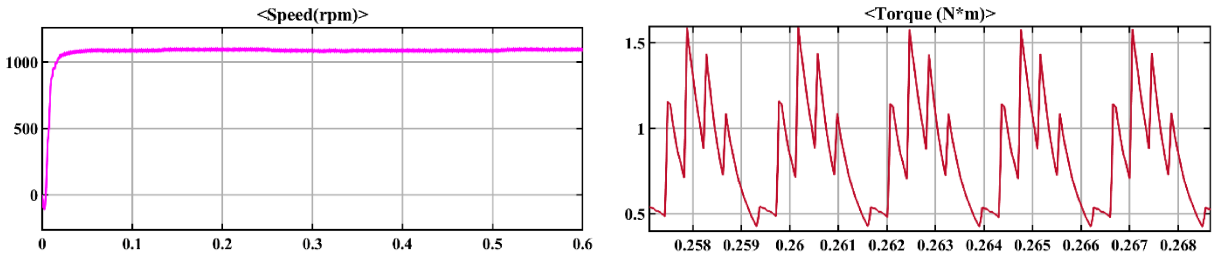


(**a**) (**b**)

Figure 5. Phase current (blue) and phase voltage (yellow) during soft commutation in motoring mode at a speed of n = 1100 rpm: (**a**) simulation results; (**b**) experimental results.

The simulation and experimental results for the phase voltage and phase current show clear similarities in amplitude and waveform. The correspondence observed between the two groups of oscillograms confirms the simulation model's accuracy in describing electromagnetic processes in the system during motoring mode operation under PWM control.

Figure 6a,b show the simulation results for the developed speed and total torque when the motor operates in the first quadrant.

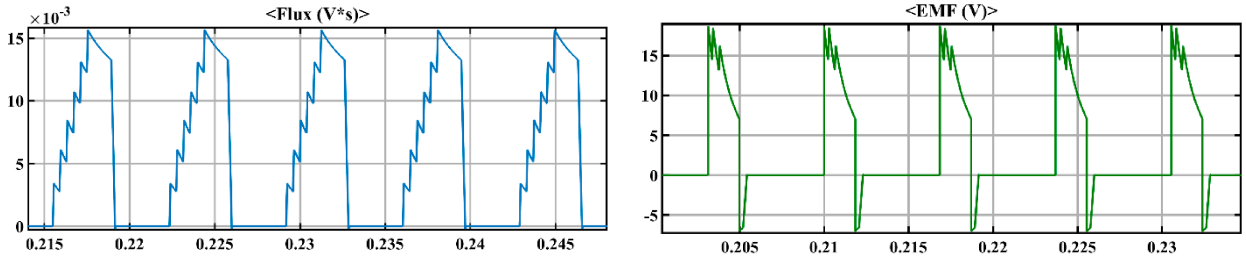


(**a**) (**b**)

Figure 6. Simulation results for unipolar modulation: (**a**) speed n [rpm]; (**b**) torque [Nm].

The resulting waveforms accurately represent the developed speed and electromagnetic torque, clearly reflecting the system's actual dynamic behavior in operating mode.

Figure 7a,b show the magnetization and back-EMF values for one of the motor phases during operation in motoring mode and under no-load conditions.

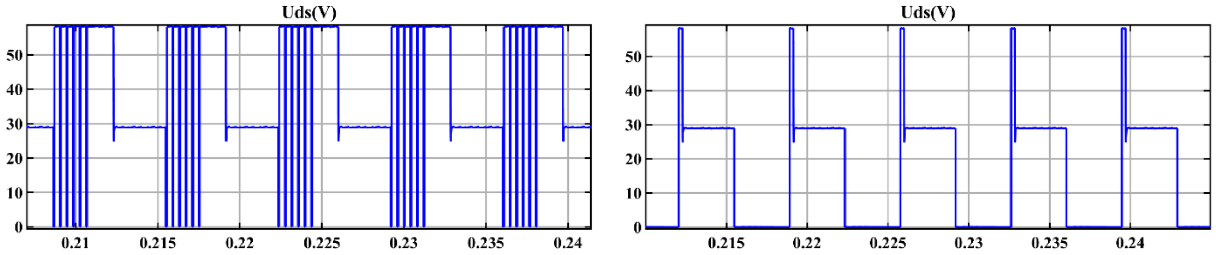


(**a**) (**b**)

Figure 7. Simulation results for unipolar modulation at a speed of n = 1100 rpm: (**a**) magnetization; (**b**) back-EMF.

Significant ripples in both the magnetization curves and the back-EMF of the motor are observed. This is characteristic of SRM operation under variable inductance. However, the magnetization follows a nearly linear variation law within the operating range under consideration. This confirms the predictability of the magnetic process and the accuracy of the used model.

Figure 8a,b illustrate the voltage U(ds) across transistors M1 and M2.

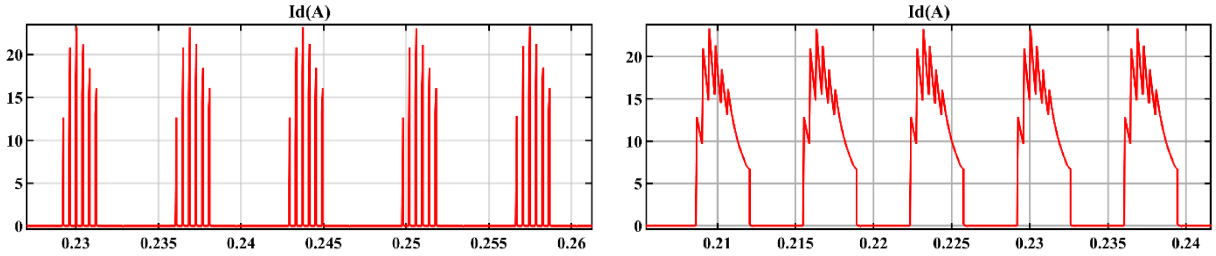


(**a**) (**b**)

Figure 8. Simulation results of the drain-source voltage U_{ds}: (**a**) transistor M1; (**b**) transistor M2.

Figure 9a,b show the current waveforms I_d for transistors M1 and M2.

https://doi.org/10.3390/engproc2026150012

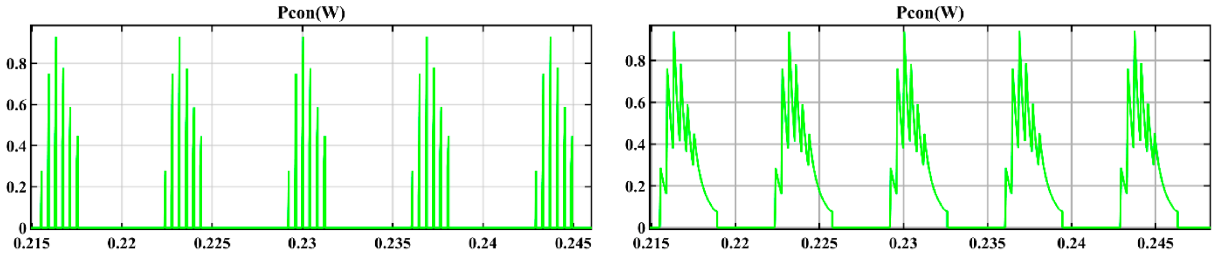


(**a**) (**b**)

Figure 9. Current I_d waveforms: (**a**) transistor M1; (**b**) transistor M2.

The observed current ripples during switching of the upper transistors confirm more stable current regulation and a more uniform electromagnetic loading under pulse width modulation (PWM) control.

Figure 10a,b show the conduction losses Pcon for transistors M1 and M2, respectively.

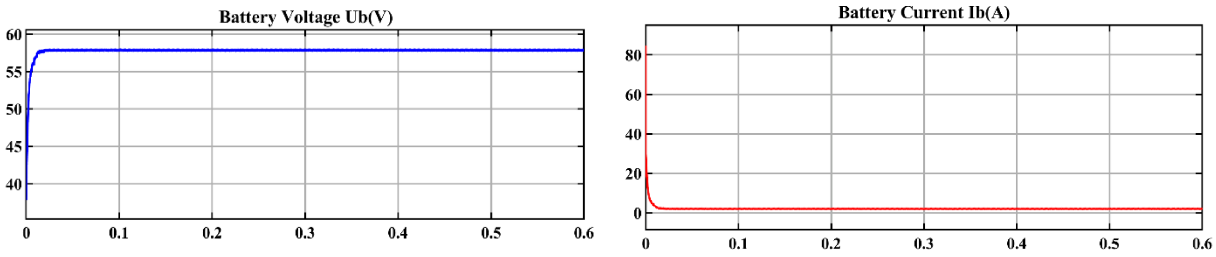


(**a**) (**b**)

Figure 10. Conduction losses Pcon: (**a**) transistor M1; (**b**) transistor M2.

The conduction losses of the upper transistors are significantly lower than those of the lower transistors due to lower current levels and shorter on-time intervals in their respective switching phases. This results in a lower heat load on the upper switches and a higher power module efficiency in the operating mode under consideration.

Figure 11a,b show the voltage and current waveforms consumed by the battery in motoring mode.



(**a**) (**b**)

Figure 11. Simulation results: (**a**) Battery voltage Ub; (**b**) Battery current Ib.

When the machine starts up, there is a distinct peak in the current drawn from the battery, which leads to a brief increase in voltage. This transient process is characteristic of the acceleration phase when the drive requires greater electromagnetic torque. Once a constant speed is reached and maintained, both the current and voltage stabilize at lower, steady levels, reflecting the normalization of the load and the establishment of steady-state operation.

https://doi.org/10.3390/engproc2026150012

3.2. Comparative Analysis of Simulation and Experimental Results

This section's comparative analysis evaluates the simulation model's accuracy against experimental measurements under various load conditions and speeds ranging from 550 to 5500 RPM. First, the relationship between load torque and speed at different effective phase current values is presented. This allows for monitoring the influence of the current on the machine's mechanical characteristics. Next, graphical comparisons are presented of the simulation and experimental results for input and output power, as well as system efficiency, as a function of speed. These comparisons enable an assessment of the model's accuracy in reproducing the energy processes in the system. Lastly, a table showing the relative error between the simulation and experimental results at a 15 A RMS phase current value is presented with respect to input power, output power, and efficiency. This enables a quantitative assessment of differences and the model's validity.

Figure 12 shows the relationship between load torque and machine speed at different RMS phase current values, enabling monitoring of the current's influence on mechanical characteristics over the entire operating range.

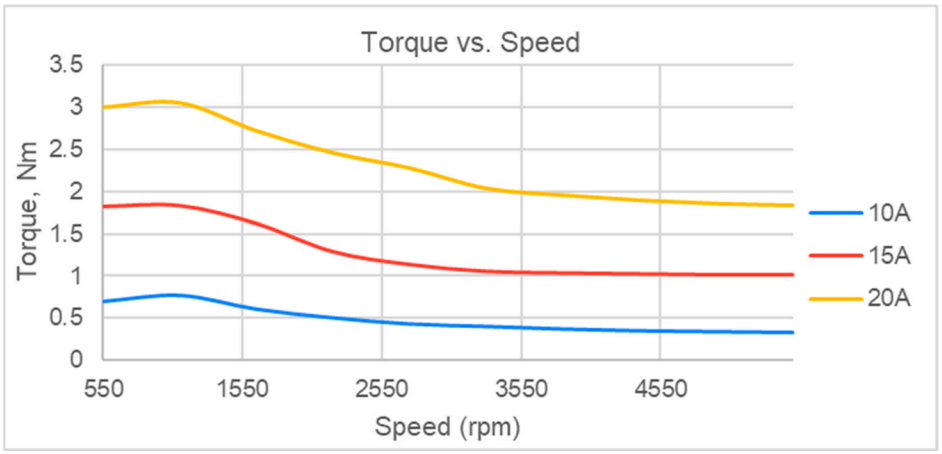


Figure 12. Experimentally obtained torque–speed curves at different current values.

As the RMS value of the phase current increases, the developed load torque increases at low and medium speeds since a higher current leads to stronger magnetization and greater electromagnetic force, as the chart clearly shows. However, at high speeds, the torque decreases despite increased current, due to the dominant influence of back-EMF and the limited time for the current to rise in the windings. This behavior is characteristic of switched reluctance motors and illustrates the limits of efficient operation at different current levels.

Figures 13 and 14 illustrate the comparison between simulation and experimental results for the variation in the machine's input and output power as a function of speed at different RMS phase-current values. These two relationships enable a direct comparison of the model and the physical machine over a wide operating range, providing an indication of how well the simulation reproduces actual energy processes under various loads and speeds.

The input power Pin indicates how the electrical load on the system changes during acceleration. The output power reflects the mechanical work the machine delivers to the load. Comparing these two quantities at different current levels allows one to assess the model's accuracy with respect to electromagnetic processes and energy efficiency.

Figure 15 shows the comparison between simulation and experimental results for the system's efficiency (%) as a function of speed for various RMS values of the phase current.

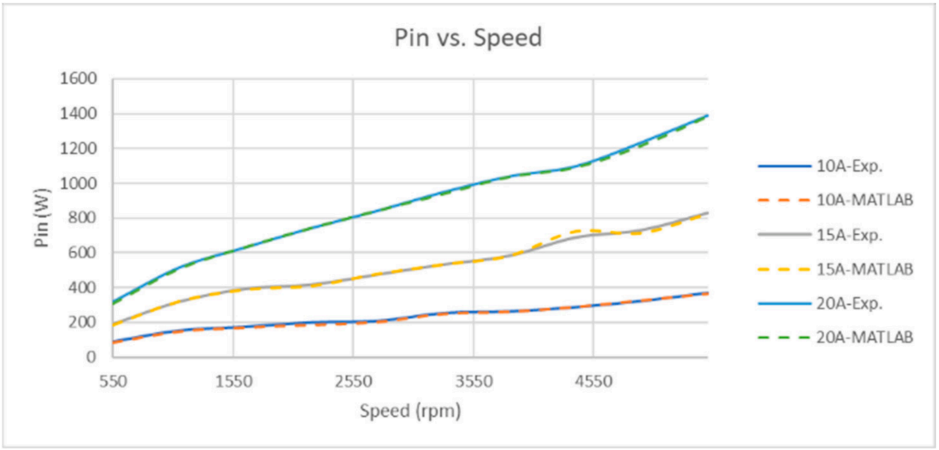


Figure 13. Input power Pin (W) as a function of motor speed n (rpm) at different current values.

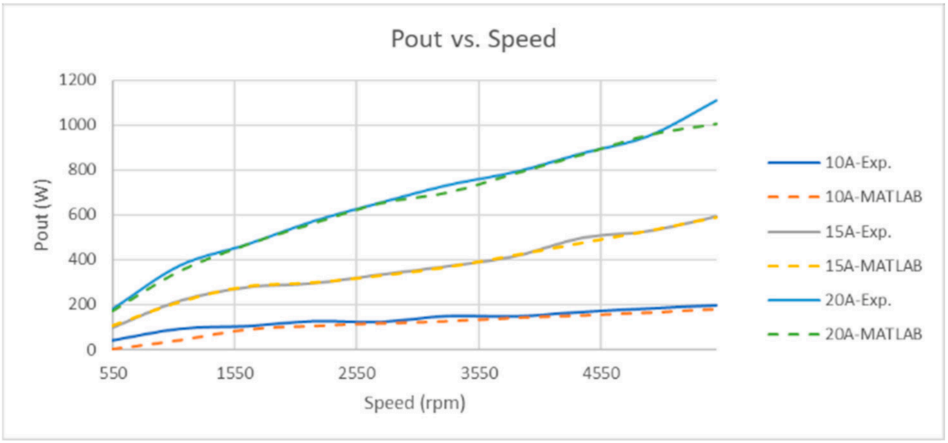


Figure 14. Output power Pout (W) as a function of motor speed n (rpm) at different current values.

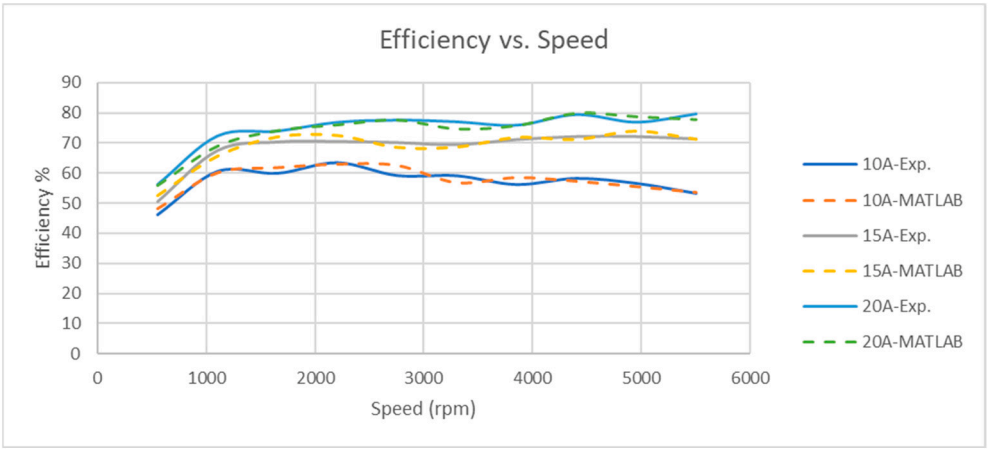


Figure 15. System efficiency as a function of machine speed and different current values.

The graphical comparison enables an assessment of the model's accuracy in describing the system's actual behavior with respect to energy conversion across the entire operating range. It should be noted that the efficiency of the SRM at low excitation currents (10 A) is affected by the friction of the bearings and the rubber sealant on the motor shaft. The efficiency increases as the motor warms up [10,11]. This phenomenon is not accounted for in the simulated results provided in the MATLAB/Simulink environment. Observed trends reveal areas where the simulation closely matches the experiment and areas where deviations arise from dynamic effects, losses, or model limitations.

Table 1 shows the difference between the simulated and experimental results for input Pin, output power Pout, and system efficiency at various speeds with an RMS phase current of 15 A.

Table 1. Relative error between the obtained simulation and experimental results for the input power Pin, output power Pout, and system efficiency.

		15A-Exp.	15A-MATLAB		15A-Exp.	15A-MATLAB		15A-Exp.	15A-MATLAB	
№	Speed [rpm]	Pin [W]	Pin [W]	Error. %	Pout [W]	Pout [W]	Error. %	Efficiency [%]	Efficiency [%]	Error. %
1	550	190.90	185.48	2.92	96.65	104.77	7.75	50.63	52.49	3.54
2	1100	320.00	321.38	0.43	216.19	210.69	2.61	67.56	65.56	3.05
3	1650	393.50	388.86	1.19	276.87	279.77	1.04	70.36	71.95	2.20
4	2200	418.00	410.03	1.94	294.82	297.04	0.75	70.53	72.45	2.64
5	2750	475.90	479.10	0.67	334.00	328.13	1.79	70.18	68.49	2.47
6	3300	534.10	533.83	0.05	371.17	366.12	1.38	69.49	68.58	1.33
7	3850	584.40	583.94	0.08	415.91	419.09	0.76	71.17	71.77	0.84
8	4400	689.70	724.33	4.78	497.62	474.35	4.91	72.15	71.13	1.44
9	4950	732.30	715.25	2.38	528.45	528.46	0.01	72.16	73.89	2.33
10	5500	830.90	825.21	0.69	593.05	587.18	1.01	71.37	71.15	0.31

The maximum relative error is 7.75%. while the minimum is 0.01%, indicating excellent agreement between the simulation and experimental results. The model's reliability and ability to reproduce the system's actual energy characteristics are confirmed by the high accuracy across a wide range of speeds and at a phase current of 15 A. These results allow us to confidently use the model to analyze and optimize performance under various operating conditions.

4. Conclusions

The paper presents a comprehensive simulation and experimental investigation of the electromagnetic, mechanical, and energy characteristics of the studied three-phase Switched Reluctance Motor over a wide range of speeds and load conditions. The analysis of the phase current and voltage oscillograms shows good agreement between the simulation model and the real system in both transient and steady-state operating modes, confirming the validity of the adopted simulation approach for describing the drive dynamics.

The obtained torque–speed characteristics at different RMS values of the phase current reflect the typical behavior of this type of motor, namely an increase in torque at low speeds and a decrease at higher speeds due to the limitations imposed by the back electromotive force and the current rise time. The comparison between simulation and experimental results for input power, output power, and efficiency demonstrates a high level of agreement, indicating that the model successfully reproduces the main energy processes in the system.

The comparative analysis based on the calculated relative error further confirms the reliability of the developed model. The minimum error is 0.01%, while the maximum remains at 7.75%, well within acceptable limits for this type of study. This indicates that the simulation model is sufficiently accurate and can be used with confidence for prediction, optimization, and analysis of motor behavior under different operating conditions.

In summary, the conducted simulation and experimental investigations demonstrate that the model adequately describes both the electrical and mechanical characteristics of the system, making it a reliable tool for future developments, control optimization, and more detailed studies of the efficiency and dynamic performance of the investigated SRM drive.

https://doi.org/10.3390/engproc2026150012

Author Contributions: T.G., G.B. and D.Y. were involved in the full process of producing this paper, including conceptualization, methodology, modeling, validation, visualization and preparing the manuscript. All authors have read and agreed to the published version of the manuscript.

Funding: The research was funded within the framework of the "A study of the Energy Exchange in a Switched Reluctance Motor System under Different Control Algorithms" project, contract № 252ПД0037-19, Scientific and Research Sector at the Technical University of Sofia.

Institutional Review Board Statement: Not applicable.

Informed Consent Statement: Not applicable.

Data Availability Statement: Data are included in the article.

Acknowledgments: This research used equipment funded by the European Regional Development Fund within the OP "Research, Innovation and Digitalization Programme for Intelligent Transformation 2021–2027", Project No. BG16RFPR002-1.014-0005 Center of competence "Smart Mechatronic, Eco-, and Energy-Saving Systems and Technologies".

Conflicts of Interest: The authors declare no conflicts of interest.

References

1. Krishnan, R. *Switched Reluctance Motor Drives: Modeling, Simulation, Analysis, Design, and Applications*; CRC Press: Boca Raton, FL, USA, 2001.
2. Husain, I. *Electric and Hybrid Vehicles: Design Fundamentals*, 2nd ed.; CRC Press: Boca Raton, FL, USA, 2011.
3. Rahman, K.; Fahimi, B.; Suresh, G.; Rajarathnam, A.; Ehsani, M. Advantages of Switched Reluctance Motor Applications to EV and HEV: Design and Control Issues. *IEEE Trans. Ind. Appl.* **2000**, *36*, 111–121. [CrossRef]
4. Mohan, N.; Undeland, T.; Robbins, W. *Power Electronics: Converters, Applications, and Design*, 3rd ed.; Wiley: Hoboken, NJ, USA, 2003.
5. Yong, L.; Jian, X. Modeling and Analysis of Asymmetric Bridge Converter for SRM Drives. *IEEE Trans. Ind. Electron.* **2006**, *53*, 1238–1247.
6. Chan, C.; Chau, K. A New Soft-Switching Converter for Switched Reluctance Motor Drives. *IEEE Trans. Power Electron.* **2001**, *16*, 428–435. [CrossRef]
7. Husain, I.; Ehsani, M. Torque Ripple Minimization in Switched Reluctance Motor Drives by PWM Current Control. *IEEE Trans. Power Electron.* **2002**, *17*, 283–290. [CrossRef]
8. Yankov, D. Investigation of a Reversible Converter Fed a Switched Reluctance Motor (SRM). Ph.D. Thesis, Technical University, Sofia, Bulgaria, 2022.
9. Yankov, D.; Grigorova, T. Analysis and Investigation of an Asymmetric Bridge Converter for a Three-Phase 12/8 SRM in Generating Mode. In Proceedings of the 2020 XI National Conference with International Participation (ELECTRONICA), Sofia, Bulgaria, 14–15 May 2020; pp. 1–4.
10. Someşan, L.; Pădurariu, E.; Husain, I.; Viorel, I.A.; Szabó, L. Simple analytical models of switched reluctance motor for design and control purpose. In Proceedings of the 2012 XXth International Conference on Electrical Machines (ICEM 2012), Marseille, France, 2–5 September 2012; pp. 2408–2413.
11. Garkal, R.B.; Rao, K. Design and implementation of switched reluctance motor. *Int. J. Adv. Eng. Res. Dev.* **2016**, *3*, 497–503.

Disclaimer/Publisher's Note: The statements, opinions and data contained in all publications are solely those of the individual author(s) and contributor(s) and not of MDPI and/or the editor(s). MDPI and/or the editor(s) disclaim responsibility for any injury to people or property resulting from any ideas, methods, instructions or products referred to in the content.